AMERICAN SOCIETY FOR MICROBIOLOGY | Molecular and Cellular Biology®

RESEARCH ARTICLE

Isc10, an Inhibitor That Links the Anaphase-Promoting Complex to a Meiosis-Specific Mitogen-Activated Protein Kinase

Abhimannyu Rimal,[a] Zeal P. Kamdar,[a] Chong Wai Tio,[a] Edward Winter[a]

[a]Department of Biochemistry and Molecular Biology, Thomas Jefferson University, Philadelphia, Pennsylvania, USA

ABSTRACT Smk1 is a meiosis-specific mitogen-activated protein kinase (MAPK) in yeast that controls spore differentiation. It is activated by a MAPK binding protein, Ssp2, upon completion of the meiotic divisions. The activation of Smk1 by Ssp2 is positively regulated by a meiosis-specific coactivator of the anaphase promoting complex (APC/C) E3 ubiquitin ligase, Ama1. Here, we identify Isc10 as an inhibitor that links APC/C^{Ama1} to Smk1 activation. Isc10 and Smk1 form an inhibited complex during meiosis I (MI). Ssp2 is produced later in the program, and it forms a ternary complex with Isc10 and Smk1 during MII that is poised for activation. Upon completion of MII, Isc10 is ubiquitylated and degraded in an *AMA1*-dependent manner, thereby triggering the activation of Smk1 by Ssp2. Mutations that caused Ssp2 to be produced before MII, or *isc10*Δ mutations, modestly reduced the efficiency of spore differentiation whereas spores were nearly absent in the double mutant. These findings define a pathway that couples spore differentiation to the G_0-like phase of the cell cycle.

KEYWORDS Ama1, Smk1, anaphase promoting complex, meiosis, mitogen-activated protein kinases, yeasts

Differentiation programs that produce specialized cells in multicellular organisms are often controlled by transcriptional cascades. Protein kinases controlled by these cascades can generate signaling networks that exist transiently as various steps in differentiation programs take place. These transitory signaling connections can define intervals when cells are able to respond to inducing signals in the environment, and they can also enforce internal dependency relationships, checkpoints, and other interactions that are unique to specific stages of a program. Despite the significance of transcriptionally regulated signaling networks for cellular differentiation, their transience makes them difficult to study, and many questions about signaling in the context of differentiation programs remain unanswered.

Sporulation is the program in yeast that most closely resembles cellular differentiation in higher eukaryotes. It is induced in a specific cell type (the diploid) by an external signal (starvation) that induces expression of a transcription factor (Ime1) (1). Ime1 activates early meiosis-specific genes that are expressed as meiotic DNA replication, homolog pairing, and genetic recombination take place (2, 3). As cells are completing recombination, the *NDT80* gene is expressed (4, 5). Ndt80 activates middle-meiosis-specific genes that are expressed as cells pass the meiotic commitment point and as meiosis I (MI) and MII are carried out (6). During MII, prospore membranes (PSMs) surround each of the incipient haploids (7). Upon completion of MII, PSMs pinch off to form four haploid cells within the mother cell. Midlate genes are induced as the multilayered spore walls are assembled within and around PSMs. Late genes are expressed during spore maturation. The end products of the program are specialized cells (spores) that are resistant to a variety of environmental insults.

Citation Rimal A, Kamdar ZP, Tio CW, Winter E. 2020. Isc10, an inhibitor that links the anaphase-promoting complex to a meiosis-specific mitogen-activated protein kinase. Mol Cell Biol 40:e00097-20. https://doi.org/10.1128/MCB.00097-20.

Address correspondence to Edward Winter, edward.winter@jefferson.edu.

Received 10 March 2020
Returned for modification 7 April 2020
Accepted 13 May 2020
Accepted manuscript posted online 18 May 2020
Published 29 July 2020

Smk1 is a tightly regulated middle-meiosis-specific mitogen-activated protein kinase (MAPK) that is required for spore morphogenesis (8, 9). Like other MAPKs, it is activated by phosphorylation of a threonine (T) and tyrosine (Y) in its T-X-Y activation motif. However, Smk1 is not phosphorylated by a MAPK kinase family member. Instead, it is phosphorylated by two mechanistically distinct reactions that take place at different stages of meiosis. First, the T-residue is phosphorylated by the CDK activating kinase, Cak1, during MI (10–12). Next, an activator protein, Ssp2, binds the monophosphorylated MAPK during MII (13, 14). Ssp2 partially activates Smk1 and thereby triggers the intramolecular autophosphorylation of Y209 to produce the fully active (doubly phosphorylated) MAPK.

Smk1 is activated long after cells pass the meiotic commitment point, and it is not directly controlled by the extracellular signals that induce the program. Instead, Smk1 activation is coupled to the completion of MII. One mechanism that prevents Smk1 activation until MII has been completed involves the translational repression of *SSP2* mRNA by a meiosis-specific RNA binding protein, Rim4 (14–17). During MII, the meiosis-specific CDK-like kinase Ime2 phosphorylates Rim4, thereby inactivating Rim4 and triggering Ssp2 translation. At this point in the program, Smk1 and Ssp2 localize to the PSMs that are growing around the incipient haploids (14). However, Ssp2 does not fully activate Smk1 until later in the program, after cells have completed anaphase II. This is because the activation of Smk1 by Ssp2 requires Ama1, a meiosis-specific coactivator of the anaphase promoting complex (APC/C) E3 ubiquitin ligase (18, 19).

Ama1 targets multiple regulatory substrates for APC/C-mediated ubiquitylation at different stages of meiotic development (20–24). It is first active in meiotic prophase when it targets mitotic cell cycle regulators (Ndd1 and Clb4) for destruction (20). This is essential for elongating prophase I, when homolog pairing and recombination take place. *ama1*Δ cells therefore carry out MI prematurely and independently of the recombination checkpoint. Despite these defects, *ama1*Δ mutants complete the meiotic divisions. However, they are defective in exiting from the cell cycle after MII has been completed (24, 25). PSMs grow around the meiotic products in the absence of *AMA1*, but they fail to pinch off, and *ama1*Δ mutant cells do not assemble spores (23, 26). Although Smk1 and Ssp2 localize to PSMs, and Smk1 is phosphorylated by Cak1 on its activation loop T in the *ama1*Δ mutant, Smk1 is underphosphorylated on Y209, and it is largely inactive (18). While the low level of active Smk1 could be an indirect consequence of the *ama1*Δ arrest, it is also possible that Ama1 directly targets an inhibitor that prevents Ssp2 from activating Smk1.

In this work, we identified a meiosis-specific protein, Isc10, as an inhibitor of Smk1 that links APC/C^{Ama1} to Smk1 activation. Our data support a model in which Isc10 binds to Smk1 during MI to form inhibited complexes. Cak1 phosphorylates the activation loop T of Smk1 at this time. During MII, the Ssp2 activator is translated and it binds to the inhibited complexes to form ternary complexes that are poised for activation. Upon completion of MII, Isc10 is degraded in an APC/C^{Ama1}-dependent manner. This allows Ssp2 to activate Smk1, triggering the autophosphorylation of the activation loop Y, thus generating the dually phosphorylated MAPK that controls spore differentiation. For simplicity, the inhibited/poised/active (IPA) model for Smk1 activation is presented in Fig. 1 and we refer to this model throughout this paper as supportive data are presented. This model explains how the transcriptional cascades of meiosis and posttranscriptional mechanisms generate MAPK complexes that connect spore differentiation to the completion of nuclear segregation. Similar interactions may play a role in controlling differentiation-specific protein kinases that connect cytodifferentiation programs to the G_0 phase of the cell cycle in multicellular organisms.

RESULTS

Ssp2 interacts with Isc10 in *ama1*Δ cells. To address the hypothesis that Ama1 regulates an inhibitor that prevents Ssp2 from activating Smk1, Ssp2 tagged with the 6×His-biotinylation site-6×His tandem affinity tag (HBH) (27) was purified from post-meiotic wild-type (WT) and *ama1*Δ cells treated or not treated with the cross-linking

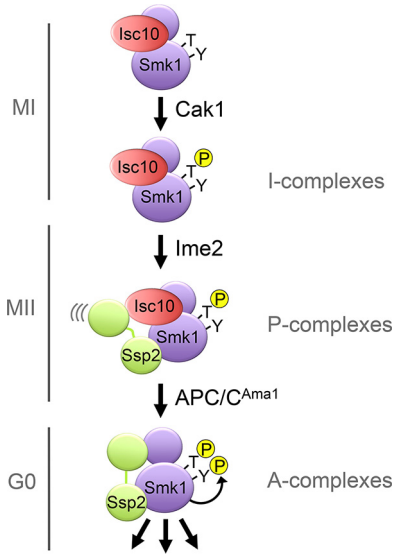

FIG 1 IPA pathway model for Smk1 activation. The model posits that different Smk1 complexes exist at different stages of meiosis. The small (ATP binding) and large (substrate binding) lobes of the MAPK are represented as purple spheres, with the activating phosphates in yellow. The newly identified inhibitor Isc10 is shown in red, and the two kinase activating segments of Ssp2 that are connected by a flexible linker are shown in green. See text for details.

reagent dithiobis(succinimidylpropionate) (DSP). Proteins were then digested with trypsin and analyzed by mass spectrometry (MS). Previous studies showed that the *ama1*Δ mutation sharply decreased the amount of Smk1 that can be copurified with Ssp2–glutathione *S*-transferase (GST) (18). However, Smk1 peptides (normalized for Ssp2-HBH peptides) were abundant in both the wild-type and *ama1*Δ samples (Table 1; see also Table S1 in the supplemental material). Thus, if Ama1 targets an inhibitor that prevents Ssp2 from activating Smk1, the inhibitor likely destabilizes the Ssp2/Smk1 interaction rather than preventing Ssp2 from binding Smk1 in the cell.

In addition to Smk1, other proteins were detected at significant levels in the wild-type and *ama1*Δ samples. One protein of interest is Isc10, a meiosis-specific protein of previously unknown function that was present at a level comparable to that of Smk1 in the *ama1*Δ sample but was present at a sharply reduced level in the wild-type sample (the normalized *ama1*Δ mutant/wild-type strain Isc10 peptide abun-

TABLE 1 Proteins cross-linked to Ssp2-HBH from postmeiotic *ama1*Δ cells ranked by iBAQ intensity[a]

Gene(s)	Protein description	iBAQ intensity		*ama1*Δ/WT iBAQ ratio
		*ama1*Δ mutant	WT strain	
SMK1	Sporulation-specific MAPK	2.6E+08	1.1E+08	2.3
ISC10	Meiosis-specific protein	1.9E+08	8.1E+06	22.7
SSA1	Heat shock protein	1.4E+08	6.8E+07	2.1
HTB1, *HTB2*	Histone H2B	7.6E+07	2.3E+07	3.3
SSA2	Heat shock protein	5.6E+07	8.4E+06	6.6
GSC2, *FKS1*	1,3-Beta-glucan synthases	5.1E+07	2.4E+06	21.2
OSW2	Outer-spore-wall protein	3.2E+07	7.6E+06	4.2
PIL1	Sphingolipid long-chain-responsive protein	2.5E+07	8.2E+06	3.0
YGR273C	Uncharacterized protein	2.4E+07	8.6E+06	2.7
PAB1	Polyadenylate binding protein	2.1E+07	8.7E+06	2.5
NOP58	Nucleolar protein 58	1.6E+07	5.9E+06	2.6
DTR1	Dityrosine transporter	1.5E+07	6.9E+05	21.2
CPR3	Peptidyl-prolyl *cis-trans* isomerase	1.4E+07	5.7E+06	2.4

[a]The intensities of cross-linked samples from wild-type (WT) cells are shown for comparison and were used to calculate severalfold enrichment in the *ama1*Δ mutant.

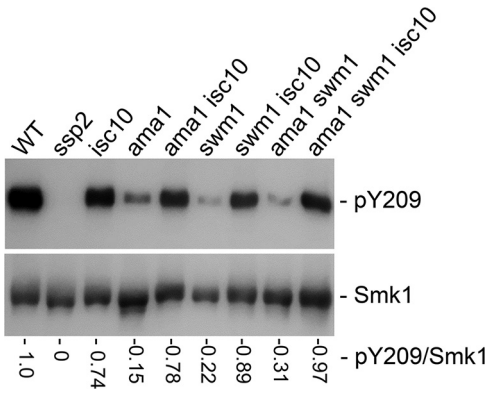

FIG 2 *isc10*Δ cells bypass the requirement of APC/C^{Ama1} for Smk1 autophosphorylation. Cells of the indicated genotypes containing a His_8-HA epitope-tagged form of Smk1 (Smk1-HH) were transferred to sporulation medium and collected at 7.5 h postinduction, when most of the cells had completed MII (68% to 75% of cells in all samples had completed MII). Cells were lysed and Smk1-HH was purified using denaturing conditions, and Smk1 and Smk1-pY209 were analyzed by immunoblotting. The pY209 levels normalized for Smk1 in the mutants are shown as a percentage of the wild-type levels (pY209/Smk1, $n = 3$).

dance ratio is 23). These findings raise the possibility that Isc10 is an inhibitor that is persistently bound to Smk1 and Ssp2 in postmeiotic *ama1*Δ cells.

In addition to Isc10, a number of other less abundant proteins were identified and some of these were overrepresented in the *ama1*Δ sample. These proteins included Gsc2 (a glucan synthase), Dtr1 (a dityrosine transporter), and Osw2 (required for spore wall assembly). All of these proteins function in spore wall morphogenesis (28–30), and Gsc2 is known to interact with Smk1 (31). These cross-linked proteins may represent targets that are associated with Smk1/Ssp2 in cells that are blocked at the *ama1*Δ arrest point. Further studies are required to test these connections. The experiments described below focus on the role of Isc10 in the Smk1 pathway.

APC/C regulates Smk1 autophosphorylation through Isc10. We hypothesized that Isc10 is an inhibitor that prevents Ssp2 from activating Smk1 in *ama1*Δ cells. If so, *isc10*Δ cells might bypass the requirement of Ama1 for Smk1 activation. To test this, the fractions of Smk1 that were autophosphorylated on the activation loop tyrosine (pY209) were compared in postmeiotic cells deleted for *AMA1* and/or *ISC10* (Fig. 2). As previously reported, the *ama1*Δ mutation substantially reduced Smk1 autophosphorylation. The *isc10*Δ mutation had a modest effect on Smk1 autophosphorylation in otherwise wild-type cells. Importantly, *isc10*Δ restored Smk1 autophosphorylation in the *ama1*Δ background. Swm1 (Apc13) is a nonessential component of the core APC/C that is required for normal spore formation (32–34). A *swm1*Δ mutation decreased the level of autophosphorylated Smk1, while the *isc10*Δ *swm1*Δ background had nearly wild-type levels. Collectively, these findings indicate that *isc10*Δ cells can bypass the requirement of the APC/C for Smk1 activation. Although Swm1 is a core subunit of the APC/C and the APC/C is essential for both mitotic and meiotic chromosome segregation, *swm1*Δ cells grow normally during vegetative growth and they complete MI and MII (32, 34). Nevertheless, *swm1*Δ mutants do not assemble normal spore walls in some genetic backgrounds (W303), and they slowly formed aberrant spore walls in the genetic background used in this study (SK1). These data raise the possibility that Swm1 plays an especially important role in promoting the Ama1-dependent function of the APC/C.

To further characterize the role of Isc10 in the Smk1 pathway, epitope-tagged forms of Smk1 and Ssp2 were monitored at various times during meiotic development in WT, *ama1*Δ, *isc10*Δ, and *ama1*Δ *isc10*Δ cells using electrophoresis through acrylamide gels containing Phos-tag, which specifically slows the migration of phosphorylated proteins (Fig. 3) (11). Smk1 and Ssp2 were undetectable in vegetative cells, and they were first detected at 5 h and 6.5 h postinduction, respectively, consistent with the activation of

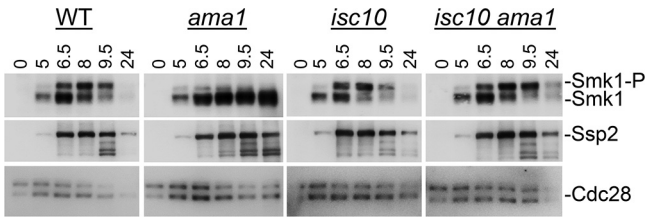

FIG 3 *isc10*Δ restores Smk1 autophosphorylation without influencing the timing or level of Smk1 or Ssp2 production. Cells of the indicated genotypes were collected at various times (in hours) postinduction and analyzed by Phos-tag–acrylamide electrophoresis and immunoblotting. Smk1 phosphorylated on T207 by Cak1 migrates in this gel system as a closely spaced doublet with unphosphorylated Smk1, while the doubly phosphorylated isoform of Smk1 migrates above (Smk1-P). Cdc28 was used as a loading control.

their promoters by Ndt80 and the translational repression of *SSP2* mRNA by Rim4 as previously described (14, 15, 35). These findings suggest that *isc10*Δ and *ama1*Δ mutations had no effect on the transcription or translation of Smk1 and Ssp2. While the slower-migrating, doubly phosphorylated form of Smk1 was barely detectable in the *ama1*Δ samples, the phosphorylation profile of Smk1 in the *isc10*Δ *ama1*Δ strain resembled the wild-type profile. These findings further support the conclusion that the *isc10*Δ mutation bypasses the requirement of Ama1 for Smk1 activation. As previously reported, Smk1 is persistent in the *ama1*Δ background (18). Whether this is because Ama1 directly regulates Smk1 stability or indirectly influences Smk1 stability by blocking the program has not been established.

Isc10 is degraded in an APC/C^{Ama1}-dependent manner. *ISC10* was previously identified as a meiosis-specific gene based on its expression (36). More-recent studies indicated that it is controlled by a middle meiotic promoter (2, 3). We analyzed the Isc10 protein tagged with the Myc epitope in meiotic time courses from wild-type, *ama1*Δ, and *swm1*Δ cells (Fig. 4A). Isc10-Myc was undetectable in vegetative cultures, and it accumulated in parallel with Smk1 starting around 5 h postinduction and reached its maximal concentration at around 6.5 h in all of the strains tested. Although the patterns

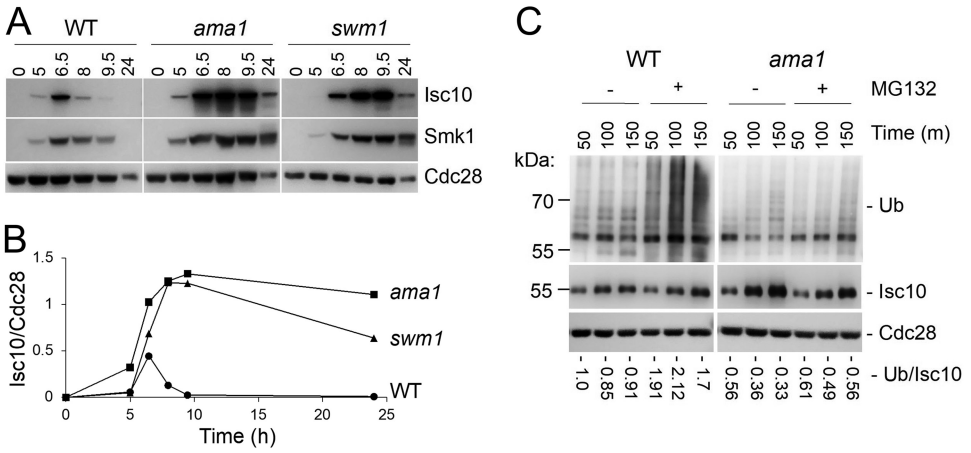

FIG 4 Isc10 is a middle-meiotic protein that is regulated by APC/C^{Ama1}. (A) *ama1*Δ and *swm1*Δ increase the level of Isc10 during meiosis. Wild-type, *ama1*Δ, and *swm1*Δ cells containing *ISC10-Myc* were transferred to sporulation medium, and samples were withdrawn at the indicated times (in hours), resolved by electrophoresis in parallel, and blotted to a single membrane that was probed with the indicated antibodies to allow the levels of Isc10 to be compared between strains. (B) Quantitation of the protein levels shown in panel A. (C) Isc10 is ubiquitylated in an *AMA1*-dependent manner. *ISC10-HBH* (WT) and *ISC10-HBH ama1*Δ cells were transferred to sporulation medium, the proteosomal inhibitor MG132 in DMSO (+) or DMSO alone (−) was added at 5.5 h postinduction as cells were completing MI, samples were withdrawn at the indicated times, and the Isc10-HBH was purified using nickel beads. Proteins were resolved by electrophoresis and blotted to a single membrane that was analyzed for Isc10-HBH or ubiquitin immunoreactivity as indicated. Cdc28 was used as a loading control. The relative amounts of ubiquitylated Isc10 were determined by dividing the total amount of ubiquitin (Ub) immunoreactivity by the Isc10 immunoreactivity.

of Isc10 and Smk1 accumulation were similar, Isc10 was present for a shorter time than Smk1 in wild-type cells. In particular, Isc10-Myc levels decreased substantially in wild-type cells between the 6.5-h and 8-h time points, when MII was being completed. Smk1 levels remained high during this interval, and they persisted until later in the program. These observations suggest that Isc10 was degraded as Smk1 activation was occuring. Importantly, the reduction in Isc10 that occurred between the 6.5-h and 8-h time points in wild-type cells was not observed in the *ama1*Δ and *swm1*Δ mutants. In addition, the overall levels of Isc10 were higher in the *ama1*Δ and *swm1*Δ cells (Fig. 4B). Taken together, these findings are consistent with Isc10 being targeted for degradation in an APC/C^{Ama1}-dependent manner and with Isc10 degradation being required for Smk1 activation (see model in Fig. 1).

To test whether Isc10 is ubiquitylated during meiosis, *ISC10-HBH* cells with and without *AMA1* were treated with a proteosome inhibitor (MG132) as MI was being completed (5.5 h postinduction). Isc10-HBH was subsequently purified using nickel beads at different times after MG132 had been added, and the purified fractions were analyzed by immunoblotting (Fig. 4C). A band of ubiquitin immunoreactivity that migrated slightly slower than the major Isc10-HBH band and ladders of higher-molecular-weight ubiquitin immunoreactivity were detected in all of the samples. MG132 treatment increased the amount of high-molecular-weight ubiquitin immunoreactivity in the wild-type samples. These immunoreactive species were reduced in the *ama1*Δ samples. These findings suggest that Isc10-HBH is polyubiquitylated in a pathway that requires APC/C^{Ama1}. The persistent Isc10-HBH observed in the *ama1*Δ background may therefore have been related to an absence of proteosomal degradation.

Isc10 interacts with Smk1 and Ssp2 in meiotic yeast cells. The kinase activating domain (KAD) of Ssp2 is located at its C terminus, and the KAD fused to glutathione *S*-transferase ($Ssp2^{KAD}$-GST) can bind Smk1 and trigger the autophosphorylation of its activation loop (13, 14). Smk1 autophosphorylation is reduced when *AMA1* is deleted from wild-type or *SSP2^{KAD}-GST* cells (18). These findings show that $Ssp2^{KAD}$-GST, which is easier to study than the full-length protein due to increased solubility, can be used to study how Ama1 controls Smk1 activation. We purified $Ssp2^{KAD}$-GST from postmeiotic wild-type, *ama1*Δ, *isc10*Δ, and *isc10*Δ *ama1*Δ cells and compared the levels of Smk1 that were present in the purified preparations (Fig. 5A). As previously reported (18), the *ama1*Δ mutation substantially reduced the amount of Smk1 that copurified with $Ssp2^{KAD}$-GST. The *isc10*Δ mutation restored the amount of copurified Smk1 in the *ama1*Δ mutant. These results, taken together with the finding that Ssp2 can be cross-linked to Smk1 in the presence or absence of *AMA1*, suggest that an Isc10/Smk1/Ssp2 complex exists in the *ama1*Δ background and that Isc10 destabilizes the interaction between Smk1 and Ssp2 (P-complexes diagrammed in Fig. 1).

We next analyzed the interaction of Smk1-HH with Isc10-Myc and $Ssp2^{KAD}$-GST (Fig. 5B). As expected, Smk1-HH purified from wild-type extracts was enriched for $Ssp2^{KAD}$-GST and was active based on the results of the pY209 autophosphorylation assay (A-complexes in Fig. 1). Isc10-Myc was undetectable in the wild-type extracts, consistent with it being degraded upon completion of meiosis. Also as expected, Smk1-HH purified from *ama1*Δ cells was inactive based on the pY209 assay. These Smk1-HH preparations were enriched for Isc10-Myc. They were also enriched for $Ssp2^{KAD}$-GST, but the level of enrichment was lower than that seen with the wild type. These findings are consistent with Smk1 existing in an inactive ternary complex with Isc10 and Ssp2 in postmeiotic *ama1*Δ cells (P-complexes in Fig. 1).

To further study the complexes, Isc10-HBH was purified with nickel beads from postmeiotic *SMK1-GST SSP2-Myc ama1*Δ cells. Smk1-GST and Ssp2-Myc were both enriched in the purified Isc10-HBH preparations (Fig. 5C). Notably, Smk1-GST was enriched to similar extents in the purified Isc10-HBH preparations from cells with and without *SSP2*. Ssp2-Myc was also enriched in the purified Isc10-HBH preparations from cells with and without *SMK1*, but the level of enrichment was higher when *SMK1* was

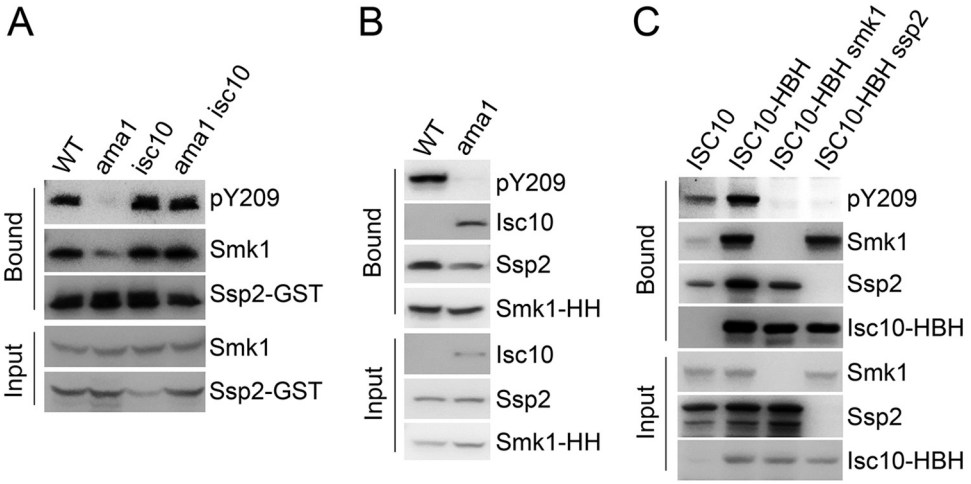

FIG 5 Isc10 interacts with Smk1 and Ssp2 in postmeiotic *ama1*Δ cells. (A) The *isc10*Δ mutant bypasses the requirement of Ama1 for formation of a stable Ssp2/Smk1 complex. Postmeiotic wild-type, *ama1*Δ, *isc10*Δ, and *ama1*Δ *isc10*Δ cells containing *SMK1-HH* and *SSP2^{KAD}-GST* were harvested 7.5 h after they had been transferred to sporulation medium. Extracts were prepared under native conditions, and Ssp2^{KAD}-GST was purified using glutathione-agarose. The bound and input fractions were analyzed by immunoblotting with the indicated antibodies. (B) Smk1-HH interacts with Ssp2 and Isc10 in *ama1*Δ cells. Postmeiotic wild-type and *ama1*Δ cells containing *SMK1-HH*, *ISC10-Myc*, and *SSP2^{KAD}-GST* were harvested and extracts prepared as described for panel A. The extracts were incubated with nickel beads to bind Smk1-HH, and the bound and input fractions were analyzed by immunoblotting with the indicated antibodies. (C) Ssp2 and Smk1 can bind to Isc10 independently. Postmeiotic *ama1*Δ cells containing *ISC10-HBH SSP2-Myc* and *SMK1-GST* were harvested and extracts prepared as described for panel A. Isc10-HBH was purified from the extracts using nickel beads, and the bound and input fractions were analyzed by immunoblotting with the indicated antibodies. The leftmost lane (*ISC10*) lacked the HBH tag and served as a negative control. All of the samples analyzed as described for this figure were from cells that had completed >75% MII as assayed by fluorescence microscopy of DAPI-stained samples.

present. These findings are consistent with the ability of Isc10 to independently bind Smk1 and Ssp2 (P-complexes in Fig. 1). As described above, Isc10 accumulates during MI in parallel with Smk1. These findings suggest that Smk1 and Isc10 interact to form a complex during MI before Ssp2 is translated (I-complexes in Fig. 1).

Isc10 interacts with Smk1 and Ssp2 in bacteria. To test whether Isc10 can directly bind Smk1 and Ssp2, a maltose binding protein (MBP)-tagged form of Isc10 (MBP-Isc10) was coexpressed with either Smk1 or Ssp2^{KAD}-GST in bacteria. The enrichment of Smk1 or Ssp2^{KAD}-GST in affinity-purified MBP-Isc10 preparations was then tested (Fig. 6A).

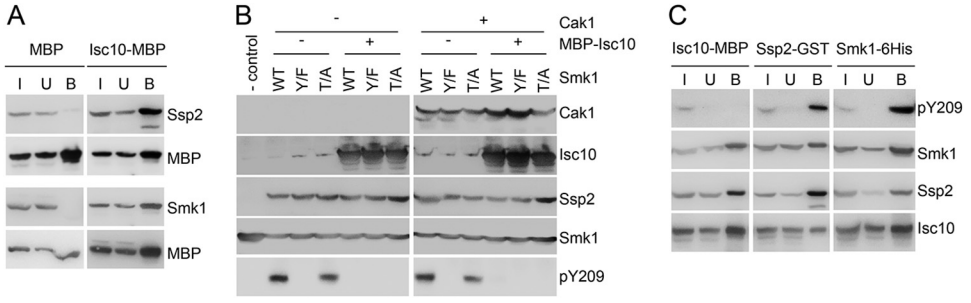

FIG 6 Reconstitution of Isc10/Smk1/Ssp2 signaling complexes in bacterial cells. (A) Isc10 can bind Smk1 independently of Ssp2 and vice versa. MBP or MBP-Isc10 was coexpressed with Ssp2^{KAD}-GST (upper two rows) or Smk1 (lower two rows) as shown. Extracts from these cells were were bound to amylose beads, and the enrichment for Smk1 or Ssp2^{KAD}-GST was analyzed in the input (I), unbound (U), and bound (B) fractions by immunoblotting. (B) Isc10 prevents Ssp2 from activating Smk1 in bacterial cells. Untagged Cak1, MBP-Isc10, or Ssp2^{KAD}-GST and untagged Smk1, Smk1-T207A (T/A), or Smk1 Y209F (Y/F) were coexpressed in bacterial cells, and total cellular extracts were analyzed with the indicated antibodies. The first lane contained extract from bacteria that expressed only Smk1 as a negative control (-control). (C) Isc10, Smk1, and Ssp2 interact in all possible combinations in the bacterial expression system. An extract of bacterial cells expressing MBP-Isc10, Ssp2^{KAD}-GST, or Smk1-HH was prepared, and these proteins were purified using amylose, glutathione, or nickel beads, respectively. Input (I), unbound (U), and bound (B) fractions were then analyzed for the indicated proteins by immunoblotting.

These experiments showed that Isc10 was able to bind Smk1 or Ssp2 independently in the absence of additional yeast factors.

Cak1 phosphorylates Smk1 on T207 and Ssp2 triggers the autophosphorylation of Smk1 on Y209 when these proteins are coexpressed in bacteria (13). We coexpressed MBP-Isc10 with Ssp2^{KAD}-GST, untagged Cak1, and untagged Smk1 in various combinations in the bacterial system (Fig. 6B). We also tested the Smk1-T207A and Smk1-Y209F mutants, which cannot be phosphorylated by Cak1 and cannot undergo autophosphorylation, respectively. As previously reported, Ssp2^{KAD}-GST activated the autophosphorylation of Smk1 on Y209 in the presence or absence of Cak1 as measured using the pY209 immunoassay. MBP-Isc10 almost completely inhibited the ability of Ssp2 to activate Smk1 autophosphorylation. These findings indicate that the presence of Isc10 is sufficient to extinguish the activation of Smk1 by Ssp2 in the absence of additional yeast factors.

We next coexpressed MBP-Isc10, Ssp2^{KAD}-GST, and Smk1-His$_6$ in bacteria and purified each of these proteins using amylose, glutathione, and nickel beads, respectively. The purified preparations were then tested for the individual proteins and autophosphorylated Smk1 (Fig. 6C). The amylose-purified MBP-Isc10 sample was enriched for both Ssp2^{KAD}-GST and Smk1-His$_6$. The Smk1-His$_6$ in these preparations was inactive as measured using the pY209 autophosphorylation assay. This purified material may have represented a mixture of Isc10/Smk1 and Isc10/Ssp2/Smk1 complexes (I- and P-complexes in Fig. 1) and an Isc10/Ssp2 complex (not diagrammed in Fig. 1). The affinity-purified Ssp2^{KAD}-GST sample also contained Smk1-His$_6$, but, in contrast to the purifed MBP-Isc10 samples, much of the Smk1-His$_6$ in these preparations was active as measured with the pY209 autophosphorylation assay. This preparation also contained some Isc10. These findings are most consistent with a fraction of the purified Ssp2^{KAD}-GST existing in a complex only with Smk1 (A-complexes), with Isc10 and Smk1 (P-complexes), and with Isc10. Purified Smk1-His$_6$ was significantly enriched for Ssp2^{KAD}-GST and Isc10, and much of the Smk1 in these preparations was autophosphorylated on Y209. While the reason that autophosphorylated Smk1 was enriched in these preparations is unclear, a possible explanation is that Isc10 sterically interferes with the interaction of Smk1-His$_6$ with the nickel affinity resin, thereby biasing the results toward recovery of A-complexes and active Smk1. Taken together, these data are consistent with the bacterial extracts containing I, P, and A complexes as diagrammed in Fig. 1.

Parallel pathways link Smk1 activation to the completion of meiosis. The *isc10*Δ mutation had no discernible effect on MI and MII as monitored by fluorescence microscopy of DAPI (4′,6-diamidino-2-phenylindole)-stained cells. Nevertheless, many of the meiotic products in *isc10*Δ cells were not surrounded by spore walls even at extended times postinduction. Thus, the fraction of these cells that contained four spores (tetrads) was reduced by 35% and the fraction of cells lacking spores or containing two spores (dyads) was increased by a corresponding fraction (Fig. 7). It has previously been reported that hyperactivation of Ime2 by deletion of its regulatory C terminus (referred to below as *IME2**) also decreased the fraction of meiotic cells that form tetrads (37), and we confirmed that this is the case in our strain background. Ime2 is known to downregulate Rim4, and Rim4 represses *SSP2* mRNA by binding to its 5′ untranslated region (UTR) (14–17, 35). One explanation for these results is that the precocious translation of Ssp2 is responsible for the decreased tetrad formation in the *IME2** strain. To address this, we placed the *SSP2* open reading frame under the control of the *SMK1* promoter (referred to below as *SSP2**), which produces Ssp2 precociously (at the same time as Smk1). *SSP2** cells completed MI and MII on schedule, but many of the meiotic products were not encapulated by spore walls and tetrad formation was reduced. These findings suggest that the precocious translation of Ssp2 is sufficient to explain the reduced tetrad/dyad ratio of *IME2**. Interestingly, the *isc10*Δ mutation in combination with either *IME2** or *SSP2** reduced tetrad formation by >90%. Taken together, these experiments indicate that the *IME2*/*RIM4*/*SSP2* pathway prevents Smk1

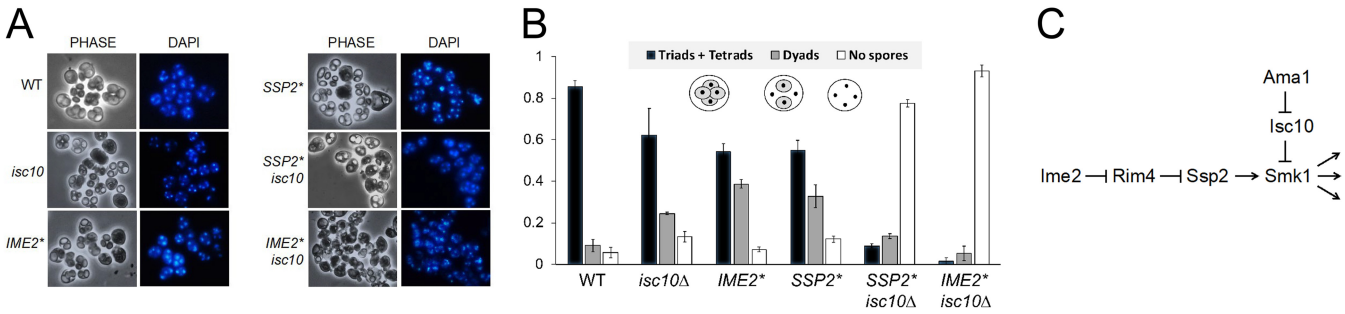

FIG 7 *ISC10* and the *IME2*/*RIM4* pathway couple spore differentiation to the completion of MII. (A) Photomicrographs of meiotic samples. Cells of the indicated genotype were incubated in sporulation medium for 36 h and stained with DAPI, and phase-contrast (PHASE) or fluorescence (DAPI) images were recorded. *IME2** indicates strains that are homozygous for the hyperactivated *IME2-ΔC241* allele, and *SSP2** indicates strains that are homozygous for the *prSMK1-SSP2* allele that produces a *SSP2* mRNA that is not translationally repressed by Rim4. (B) Quantitation of spore differentiation. Cells that had completed MII were scored for the presence of tetrads or triads, dyads, and no detectable spores/monads. Greater than 85% of the cells completed MII in all cases. The data represent averages of results from 100 cells in experiments performed in triplicate. (C) A model for the genetic interactions tested in these experiments. See text for details.

activation until MII is under way by delaying translation of Ssp2 and that Isc10 prevents Ssp2 from activating Smk1 until MII has been completed. We propose that both of these pathways delay Smk1 activation and spore morphogenesis until cells have completed the meiotic divisions and entered the G_0-like phase of the cell cycle (Fig. 7C). These pathways thereby couple spore differentiation to the G_0-like phase of the cell cycle.

DISCUSSION

This study was motivated by the finding that Ama1 promotes activation of the Smk1 MAPK (18, 19). On the basis of this observation, Isc10 was identified as an inhibitor that couples APC/C^{Ama1} to Smk1 activation. Our findings show that Isc10 prevents Smk1 activation until MII has been completed and support the IPA model diagrammed in Fig. 1. In this model, Smk1 and Isc10 are produced as cells enter MI. Cak1 phosphorylates Smk1's activation loop during MI (whether Cak1 has a preference for free Smk1 or for Smk1 that is bound by Isc10 is not known). Smk1-pT207/Isc10 (I-complexes) are catalytically inactive not only because they are bound by the Isc10 inhibitor but also because Ssp2, which is essential for kinase activation, has not yet been translated. During MII, PSMs grow around the incipient haploids. Ime2 phosphorylates the Rim4 translational repressor during MII, and this triggers the translation of a set of mRNAs that includes Ssp2 mRNA. Ssp2 colocalizes with Smk1-pT207 and Isc10 at PSMs to form complexes that are poised for activation (P-complexes). In this model, APC/C^{Ama1} is required for ubiquitin-dependent proteosomal destruction of Isc10 upon completion of MII. This allows Ssp2 to activate Smk1, which then autophosphorylates Y209 to generate the doubly phosphorylated high-activity form of the kinase (A-complexes) that controls spore differentiation.

Previous studies have shown that Ssp2 in A-complexes interacts with Smk1 via two domains that resemble RNA recognition motifs (kinase activating RRM-like motifs, or KARLS, are indicated as green spheres in Fig. 1) (38). Although KARLs 1 and 2 can bind Smk1 independently, binding of both KARLs is required for Smk1 activation. This study raises the possibility that Isc10 in P-complexes specifically prevents one of the KARLs from interacting with Smk1. If so, the Ssp2/Smk1 interaction in P-complexes is expected to be less stable than the Ssp2/Smk1 interaction in A-complexes since the binding affinity in A-complexes would approximate the product of the individual KARL/Smk1 binding affinities. This could explain why less Smk1 was recovered with $Ssp2^{KAD}$-GST from postmeiotic *ama1*Δ cells than from wild-type cells. According to this model, Ssp2, Smk1, and Isc10 form a switch in P-complexes in which one of the KARLs binds Smk1 and the second KARL is poised to engage the MAPK and activate catalysis upon downregulation of Isc10 (Fig. 1, middle panel).

Cells that lacked the Isc10 inhibitor and that also precociously produced the Ssp2

activator (*SSP2* isc10*Δ and *IME2* isc10*Δ cells) completed MII, and yet most of these meiotic products were not surrounded by spore walls. Thus, mutants that lack Smk1 activity and mutants that precociously activate Smk1 form defective spores. These findings demonstrate that Smk1 activation must be delayed until the meiotic divisions have been completed and highlight the importance of coordinating activation of the Smk1 MAPK with the cell cycle.

According to the IPA model, Ama1 triggers Smk1 activation. The regulation of Ama1 during meiotic development is complex (20–24, 39, 40). As described above, it superimposes meiotic regulation on prophase. At the same time, its activity toward proteins such as securin is inhibited by a regulatory subunit of the APC/C, Mnd2 (21, 22). In addition, Ama1 is inhibited by the M-phase form of CDK. As cells complete MII, Ama1 is activated, likely by inhibition of Mnd2 and by the removal of inhibitory phosphates from Ama1 itself. The translation of Ama1 mRNA is also upregulated at this time, and this plays an essential role in inducing cell cycle exit following MII (24, 41, 42). This is the point in the program when Isc10 is degraded and Smk1 is activated, suggesting a mechanism for coupling activation of the MAPK to the G_0 phase of the cell cycle.

Although the *isc10*Δ mutation bypasses the requirement of *AMA1* for Smk1 activation, both the single *ama1*Δ mutants and double *ama1*Δ *isc10*Δ mutants blocked meiotic development shortly after MII had been completed. Indeed, the *ama1*Δ and *ama1*Δ *isc10*Δ phenotypes were indistinguishable in analysis by light microscopy. Thus, proteins in addition to Isc10 must be downregulated by APC/C^{Ama1} to allow completion of the program. It has been proposed that Ama1 targets the Ndt80 transcription factor and the Cdc5 polo-like kinase and that this plays an essential role in promoting exit from the cell cycle following MII (24). It has also been proposed that Ama1 targets SspI, a component of the leading edge of the PSM, for destruction after MII has been completed and that this plays a role in closing the membrane around the haploid products (26). Further studies are required to define the essential set of APC/C^{Ama1} targets that control exit from MII and spore formation.

Cytodifferentiation typically takes place in the G_0 phase of the cell cycle. Although the mechanisms that couple cytodifferentiation to G_0 are incompletely understood, it is known that APC/C^{Cdh1}, which is activated upon completion of the M phase, can play a role in this process in multicellular organisms (43). While the role of Cdh1 has been best studied during neuronal differentiation, Cdh1 also appears to be important in coupling other differentiation programs to the cell cycle by influencing the length of the G_1 phase and also by regulating transcription and signaling once a cell is in G_0. Cdh1 is downregulated during meiotic development in yeast (44), and it plays no obvious role in controlling spore formation. Ama1 and Cdh1 are similar in several respects. They share similar amino acid sequences and perform similar biochemical functions, and they are both inactivated during M phases and upregulated as cells complete chromosome segregation. In addition, they both connect differentiation to the G_0 phase of the cell cycle. These connections make targets of Cdh1 that inhibit MAPKs and MAPK-like kinases attractive candidates for coupling differentiation to the G_0 phase of the cell cycle in multicellular organisms.

MATERIALS AND METHODS

Yeast strains and culture conditions. All yeast strains used in this study were in the SK1 background (Table 2). Cells were grown in YEPD (1% yeast extract, 2% peptone, 2% glucose) supplemented with adenine to 40 μg/ml or with SD (0.67% yeast nitrogen base without amino acids, 2% glucose, and nutrients essential for auxotrophic strains) at 30°C. Sporulation assays were performed by inoculating cells from YEPD into YEPA (1% yeast extract, 2% peptone, 2% potassium acetate) supplemented with adenine to 40 μg/ml and growing them overnight at 30°C to a density of 10^7 cells/ml. Cells were pelleted by centrifugation, washed, and resuspended in sporulation medium (2% potassium acetate, 10 μg/ml adenine, 5 μg/ml histidine, 30 μg/ml leucine, 7.5 μg/ml lysine, 10 μg/ml tryptophan, 5 μg/ml uracil) at 1.5×10^7 cells/ml and incubated in a roller drum at 30°C.

To construct the *SSP2-HBH* strains, three overlapping PCR fragments containing the C-terminal coding sequence of *SSP2*, pFA6a-HBH-*TRP1*, and the 3′ UTR of *SSP2* were joined by PCR and this fragment was used to transform haploid yeast strains that were used to generate JTY133 and ARY106 by standard genetic methods. To construct the *ISC10-HBH* strains, three overlapping PCR fragments containing the C-terminal coding sequence of *ISC10*, pFA6a-HBH-hphMX4, and the 3′ UTR sequence of *ISC10* were

TABLE 2 Yeast strains used in this study

Strain	Genotype[a]	Reference or source
JTY4	*MAT***a**/*MAT*α *SMK1-HH::LEU2/SMK1-HH::LEU2 ssp2Δ/ssp2Δ*	11
JTY133	*MAT***a**/*MAT*α *SMK1-3HA::HIS3/SMK1-3HA::HIS3 SSP2-HBH::TRP1/SSP2-HBH::TRP1 his3Δ/his3Δ*	This study
ARY106	*MAT***a**/*MAT*α *SMK1-3HA::HIS3/SMK1-3HA::HIS3 ama1::HIS3/ama1::HIS3 SSP2-HBH::TRP/SSP2-HBH::TRP1 his3Δ/his3Δ*	This study
ARY107	*MAT***a**/*MAT*α *SMK1-HH::LEU2/SMK1-HH::LEU2 isc10::kanMX4/isc10::kanMX4*	This study
ARY108	*MAT***a**/*MAT*α *SMK1-HH::LEU2/SMK1-HH::LEU2 isc10::kanMX4/isc10::kanMX4 ama1::TRP1/ama1::TRP1*	This study
ARY109	*MAT***a**/*MAT*α *SMK1-HH::LEU2/SMK1-HH::LEU2 swm1::kanMX4/swm1::kanMX4*	This study
ARY110	*MAT***a**/*MAT*α *SMK1-HH::LEU2/SMK1-HH::LEU2 swm1::kanMX4/swm1::kanMX4 ama1::TRP1/ama1::TRP1*	This study
ARY111	*MAT***a**/*MAT*α *SMK1-HH::LEU2/SMK1-HH::LEU2 isc10::kanMX4/isc10::kanMX4 swm1::kanMX4/swm1::kanMX4*	This study
ARY112	*MAT***a**/*MAT*α *SMK1-HH::LEU2/SMK1-HH::LEU2 ama1::TRP1/ama1::TRP1 isc10::kanMX4/isc10::kanMX4 swm1::kanMX4/swm1::kanMX4*	This study
ARY113	*MAT***a**/*MAT*α *SMK1-HH::LEU2/SMK1-HH::LEU2 isc10::kanMX4/isc10::kanMX4 SSP2-13Myc::kanMX6/SSP2-13Myc::kanMX6*	This study
ARY114	*MAT***a**/*MAT*α *SMK1-HH::LEU2/SMK1-HH::LEU2 ama1::TRP1/ama1::TRP1 SSP2-13Myc::kanMX6/SSP2-13Myc::kanMX6 isc10::kanMX4/isc10::kanMX4*	This study
ARY117	*MAT***a**/*MAT*α *SMK1-HH::LEU2/SMK1-HH::LEU2*	This study
ARY118	*MAT***a**/*MAT*α *SMK1-HH::LEU2/SMK1-HH::LEU2 ama1::TRP1/ama1::TRP1*	This study
ARY119	*MAT***a**/*MAT*α *SMK1-HH::LEU2/SMK1-HH::LEU2 SSP2-13Myc::kanMX6/SSP2-13Myc::kanMX6*	This study
ARY120	*MAT***a**/*MAT*α *SMK1-HH::LEU2/SMK1-HH::LEU2 ama1::TRP1/ama1::TRP1 SSP2-13Myc::kanMX6/SSP2-13Myc::kanMX6*	This study
ARY121	*MAT***a**/*MAT*α *SMK1-HH::LEU2/SMK1-HH::LEU2 ISC10-13Myc::hphMX4/ISC10-13Myc::hphMX4*	This study
ARY122	*MAT***a**/*MAT*α *SMK1-HH::LEU2/SMK1-HH::LEU2 ama1::TRP1/ama1::TRP1 ISC10-13Myc::hphMX4/ISC10-13Myc::hphMX4*	This study
ARY125	*MAT***a**/*MAT*α *SMK1-HH::LEU2/SMK1-HH::LEU2 ISC10-13Myc::hphMX4/ISC10-13Myc::hphMX4 SSP2-Δ137-GST::TRP1/SSP2-Δ137-GST::TRP1*	This study
ARY126	*MAT***a**/*MAT*α *SMK1-HH::LEU2/SMK1-HH::LEU2 ISC10-13Myc::hphMX4/ISC10-13Myc::hphMX4 ama1::TRP1/ama1::TRP1 SSP2-Δ137-GST::TRP1/SSP2-Δ137-GST::TRP1*	This study
ARY131	*MAT***a**/*MAT*α *SMK1-HH::LEU2/SMK1-HH::LEU2 SSP2-Δ137-GST::TRP1/SSP2-Δ137-GST::TRP1*	This study
ARY132	*MAT***a**/*MAT*α *SMK1-HH::LEU2/SMK1-HH::LEU2 SSP2-Δ137-GST::TRP1/SSP2-Δ137-GST::TRP1 ama1::TRP1/ama1::TRP1*	This study
ARY133	*MAT***a**/*MAT*α *SMK1-HH::LEU2/SMK1-HH::LEU2 isc10::kanMX4/isc10::kanMX4 SSP2-Δ137-GST::TRP1/SSP2-Δ137-GST::TRP1*	This study
ARY134	*MAT***a**/*MAT*α *SMK1-HH::LEU2/SMK1-HH::LEU2 SSP2-Δ137-GST::TRP1/SSP2-Δ137-GST::TRP1 isc10::kanMX4/isc10::kanMX4 ama1::TRP1/ama1::TRP1*	This study
ARY127	*MAT***a**/*MAT*α *SMK1-GST::kanMX6/SMK1-GST::kanMX6 SSP2-13Myc::kanMX6/SSP2-13Myc::kanMX6 ama1::TRP1/ama1::TRP1*	This study
ARY129	*MAT***a**/*MAT*α *SMK1-GST::kanMX6/SMK1-GST::kanMX6 SSP2-13Myc::kanMX6/SSP2-13Myc::kanMX6 ama1::TRP1/ama1::TRP1 ISC10-HBH::hphMX4/ISC10-HBH::hphMX4*	This study
ARY136	*MAT***a**/*MAT*α *smk1::LEU2/smk1::LEU2 SSP2-13Myc::kanMX6/SSP2-13Myc::kanMX6 ama1::TRP1/ama1::TRP1 ISC10-HBH::hphMX4/ISC10-HBH::hphMX4*	This study
ARY138	*MAT***a**/*MAT*α *SMK1-GST::kanMX6/SMK1-GST::kanMX6 SSP2-13Myc:URA3::kan/SSP2-13Myc:Ura3::kan ama1::TRP1/ama1::TRP1 ISC10-HBH::hphMX4/ISC10-HBH::hphMX4*	This study
ARY157	*MAT***a**/*MAT*α *ISC10-HBH::hphMX4/ISC10-HBH::hphMX4 pdr5::TRP1/pdr5::TRP1*	This study
ARY158	*MAT***a**/*MAT*α *ISC10-HBH::hphMX4/ISC10-HBH::hphMX4 pdr5::TRP1/pdr5::TRP1 ama1::TRP1/ama1::TRP1*	This study
ZKY12	*MAT***a**/*MAT*α *SMK1-HH::LEU2/SMK1-HH::LEU2 swm1::kanMX4/swm1::kanMX4 ISC10-13Myc::hphMX4/ISC10-13Myc::hphMX4*	This study
ZKY14	*MAT***a**/*MAT*α *isc10::kanMX4/isc10::kanMX4 ime2-Δc241-HA6::kanMX6/ime2-Δc241-HA6::kanMX6*	This study
ZKY15	*MAT***a**/*MAT*α *SMK1-HH::LEU2/SMK1-HH::LEU2 leu2::pSMK1-SSP2-GST::TRP1/leu2::pSMK1-SSP2-GST::TRP1*	This study
ZKY17	*MAT***a**/*MAT*α *SMK1-HH::LEU2/SMK1-HH::LEU2 isc10::kanMX4/isc10::kanMX4 leu2::pSMK1-SSP2-GST::TRP1/leu2::pSMK1-SSP2-GST::TRP1*	This study
608	*MAT***a**/*MAT*α *ime2-Δc241-HA6::kanMX6/ime2-Δc241-HA6::kanMX6*	37
ZKY35	*MAT***a**/*MAT*α *his4/his4*	This study
ZKY41	*MAT***a**/*MAT*α *his4/his4 isc10::kanMX4/isc10::kanMX4*	This study

[a]The genetic background for all strains in this table was SK1 carrying the following markers: *ura3 leu2::hisG trp1::hisG lys2 ho::LYS2*. The strains were phenotypically His negative and were *his4* and/or *his3* except where the *HIS* genotype is indicated.

joined by PCR and this fragment was used to transform haploid yeast strains that were used to generate ARY129, ARY136, ARY138, ARY157, and ARY158 by standard genetic methods. The HBH fragments were generated using plasmids described by Tagwerker et al. as the templates (45) (Addgene plasmids 26874 and 26873). To construct the *ISC10-13Myc* strain, four overlapping PCR fragments containing the C-terminal coding sequence of *ISC10*, pFA6a-13Myc, hphMX4, and the 3′ UTR sequence of *ISC10* were

TABLE 3 Plasmids used in this study

Plasmid	Description	Reference or source
pJT72	pET-30b + SMK1	13
pJT111	pETDuet-1 + SSP2ΔN137-GST	13
pJT115	pETDuet-1 + SSP2ΔN137-GST + SMK1	13
pJT122	pACYCDuet-1 + CAK1	13
pJT128	pETDuet-1 + SSP2ΔN137-GST + SMK1-Y209F	13
pJT130	pETDuet-1 + SSP2ΔN137-GST + SMK1-T207A	13
pJT132	pETDuet-1 + SSP2ΔN137-GST + SMK1-6HIS	13
pTP47	pETDuet-1 + MBP-Pre-SSP2^{co}ΔN265	This study
pZK6	pACYCDuet-1 + MBP-Pre-ISC10^{co}	This study
pZK11	pACYCDuet-1 + MBP-Pre	This study
pZK12	pACYCDuet-1 + MBP-Pre-ISC10^{co} + CAK1	This study

joined by PCR and this fragment was used to transform haploid yeast strains that were used to generate diploid strains ARY121, ARY122, ARY125, ARY126, and ZKY12 by standard genetic methods. The 13Myc-kanMX6 fragment used for this overlapping PCR was generated using a plasmid described by Bahler et al. as a template (Addgene plasmid 39294) (46). To construct *isc10*::*kan* and *swm1*::*kan* deletion strains, PCR fragments generated from the YKO deletion strain collection (47) using primers corresponding to sequences approximately 250 bp upstream and downstream of the replaced open reading frames (ORFs) were used to transform haploid yeast strains that were used to generate ARY107, ARY108, ARY109, and ARY110 by standard genetic methods.

Plasmids. Plasmids used in this study are listed in Table 3. Smk1, Smk1-T207A, Smk1-Y209F, Smk1-HH, Cak1, and Ssp2^{KAD}-GST (*SSP2ΔN137-GST*) were expressed in *Escherichia coli* strain BL21(DE3) in various combinations using the pET-DUET-1 coexpression plasmid system as previously described (13). To produce Isc10 in this system, a full-length *ISC10* gene was synthesized with codon optimization for *E. coli* expression (*ISC10^{CO}* sequence available upon request) by GenScript Biotech Corporation. The plasmid used to produce a MBP-*ISC10^{CO}* fusion with the elements of the fusion separated by a PreScission protease (Pre) site was constructed in 3 steps. In the first step, a PCR fragment containing MBP-Pre-*SSP2$^{265-371}$* flanked by NotI and NcoI sites was generated using plasmid pTP47 as a template. This fragment was digested and subcloned into similarly digested pACYC-Duet-1 (Novagen). In the second step, the NheI restriction endonuclease site located at nucleotide 1752 in the pACYC-Duet vector was removed using site-directed mutagenesis. In the third step, the resulting plasmid was digested with NheI (located between MBP and *SSP2* coding sequences) and NotI (located downstream of *SSP2* in the polylinker) and ligated to a similarly digested *ISC10^{CO}* PCR fragment with its initiator ATG contained within an NheI site and a NotI site located after its termination codon, generating pZK6. pZK11 was constructed by subcloning a MBP-Pre PCR fragment flanked by NotI and NcoI sites from pTP47 into a similarly digested pACYC-Duet-1 vector. To construct the plasmid that directs the production of both Cak1 and MBP-*ISC10*, the *CAK1* coding sequence was excised from pJT122 by digestion with AflII and XhoI and this fragment was ligated into similarly digested pZK6 to produce pZK12. The insertions in all of these plasmids were sequenced in their entirety.

Ssp2-HBH cross-linking and tandem affinity denaturing purification. A total of 2.5×10^9 cells per strain were collected at 7 h 15 min and 8 h 15 min after transfer to sporulation medium and were washed in 1× phosphate-buffered saline (PBS), resuspended in 1× PBS, and split in half. One half of each sample from each time point was treated with dithiobis(succinimidyl propionate) (DSP) in dimethyl sulfoxide (DMSO) to reach a final concentration of 2 mM, and the other half was treated with an equal volume of DMSO. The samples were incubated at room temperature for 40 min on a rocking platform, and the reaction was quenched by the addition of Tris (pH 7.4) to reach a 20 mM final concentration and incubated for an additional 15 min at room temperature. Cells were collected by centrifugation and frozen at −80°C. The sample was thawed on ice, resuspended in lysis buffer (8 M urea, 300 mM NaCl, 0.5% NP-40, 50 mM sodium phosphate, 50 mM Tris-Cl, pH 8.0) supplemented with protease inhibitors at the concentrations specified (48) and disrupted using three 40-s pulses of a model 24 Mini-Beadbeater with 1 min cooling on ice in between pulses. The 7 h 15 min and 8 h 15 min samples were pooled, and the proteins were purified by tandem affinity purification as described previously (49). In brief, proteins were first purified using nickel beads and eluted with a low-pH buffer containing EDTA. The pH was readjusted, and the samples were loaded onto streptavidin beads, washed extensively with 2% SDS, and stored in ammonium carbonate at 4°C.

Mass spectrometry analyses. Trypsin digestion was performed on beads, and the digests were analyzed by liquid chromatography-tandem mass spectrometry (LC-MS/MS) on a Q Exactive HF mass spectrometer (Wistar proteomics facility). MS/MS spectra generated from the LC-MS/MS runs were searched using full tryptic specificity against the UniProt *Saccharomyces cerevisiae* database plus the Ssp2-HBH sequence using the MaxQuant 1.6.0.16 program. Protein quantification was performed using unique plus razor peptides (nonunique peptides assigned to the most abundant protein group). False-discovery rates for protein and peptide were set at 1%.

Protein levels (expressed as intensity-based absolute quantification [iBAQ] values) from the cross-linked (+DSP) WT and *ama1*Δ samples were normalized for Ssp2-HBH levels (Table 1; see also Table S1 in the supplemental material). iBAQ intensities equal to zero in each data set were substituted with the lowest detectable iBAQ intensity for that sample to calculate the severalfold enrichment relative to the

negative-control (-DSP) sample. False positives, defined as proteins that showed less than 3-fold enrichment, were filtered out. The remaining hits were ranked by decreasing iBAQ abundance in the *ama1*Δ samples (Table 1). The iBAQ abundance values for those hits in the wild-type sample are also shown for comparison. The severalfold change enrichment values representing cross-linked hits from the *ama1*Δ samples relative to the WT samples were calculated to identify candidate proteins that were enriched in the *ama1*Δ samples.

Purification of proteins. To prepare total cellular extracts for immunoblotting, cells were lysed with NaOH, and proteins were precipitated with trichloroacetic acid (TCA) and solubilized with 8 M urea as described previously (50). This protocol maximizes extraction of membrane-associated proteins from TCA precipitates and has been shown to result in efficient extraction of proteins from PSMs.

Smk1 tagged with His_8 and the hemagglutinin (HA) epitope (Smk1-HH) was purified under denaturing conditions as previously described (11). In brief, 2×10^8 cells were collected by centrifugation and lysed with 2 M NaOH. Proteins were precipitated with TCA, washed with acetone, resuspended in denaturing buffer (6 M guanidine hydrochloride, 100 mM $NaHPO_4$, 10 mM Tris-Cl, pH 8.0), and purified using nickel beads. Samples were eluted in sample buffer containing 200 mM imidazole and were analyzed by gel electrophoresis.

Purification of $Ssp2^{KAD}$-GST was performed as described previously (14). Briefly, 5×10^8 cells were collected by centrifugation and resuspended in 1 ml of lysis buffer (150 mM NaCl, 5 mM $MgCl_2$, 25 mM Tris-Cl, pH 7.4) and protease inhibitors. The cells were lysed using three 40-s and one 30-s pulses of a model 24 Mini-Beadbeater with 1 min of cooling on ice between pulses, and NP-40 was added to reach a final concentration of 0.5%. A low-speed centrifugation step was used to separate the whole-cell extract from the beads, and centrifugation at 15,000 rpm and 4°C for 10 min was used to clarify the lysates. Lysates were added to 80 μl of glutathione-Sepharose 4B, and the resulting mixture incubated for 4 h at 4°C with end-over-end rotation. The beads were washed 4 times with lysis buffer and eluted with 25 mM reduced glutathione–25 mM Tris HCl (pH 7.4). The eluted proteins were precipitated with trichloroacetic acid (TCA), washed with acetone, and analyzed by gel electrophoresis.

To purify Isc10-HBH and Smk1-HH proteins under native conditions, 5×10^8 cells were collected using centrifugation and resuspended in 1 ml of lysis buffer (300 mM NaCl, 5 mM $MgCl_2$, 50 mM Tris-Cl, pH 8.0) containing protease inhibitors. The cells were lysed, NP-40 was added, and clarified lysates were prepared by centrifugation as described in the preceding paragraph. Lysates were added to 100 μl of nickel-nitrilotriacetic acid (Ni-NTA)–agarose and incubated with end-over-end rotation for 4 h at 4°C. The beads were washed four times with lysis buffer, boiled in sample buffer containing 200 mM imidazole, and analyzed by gel electrophoresis.

MG132 treatment and Isc10 ubiquitylation. MG132 in DMSO or an equivalent volume of DMSO was added to *ISC10-HBH pdr5*Δ cells with or without *AMA1* 5.5 h after they had been transferred to sporulation medium, when approximately 50% of the cells had completed MI. The cells were incubated at 30°C for various intervals, collected by centrifugation, and lysed with 2 M NaOH. Proteins were precipitated with TCA, resuspended in denaturing buffer (6 M guanidine hydrochloride, 100 mM $NaHPO_4$, 10 mM Tris-Cl, pH 8.0), purified using nickel beads, eluted in sample buffer containing 200 mM imidazole, and analyzed by gel electrophoresis.

Immunoblotting. Samples were resolved by electrophoresis on 8% acrylamide gels. Proteins were transferred to Immobilon-P membranes and probed with mouse anti-HA.11 (1:10,000), mouse anti-Myc (1:5,000), or mouse anti-GST (1:500). Smk1-pY209 analyses were performed as previously described (11). Mouse PSTAIR antibody (Sigma; 1:10,000) was used to detect Cdc28p as loading control, and a rabbit antiubiquitin antiserum (Dako; 1:500) was used to detect ubiquitylated proteins. Horseradish peroxidase (HRP)-conjugated goat anti-mouse immunoglobulin G antibody (1:7,500) or HRP-conjugated anti-rabbit antibody (1:5,000) was used as a secondary antibody. Streptavidin-conjugated HRP (1:7,500) was used to detect HBH-tagged proteins.

Protein samples analyzed using Phos-tag–acrylamide gels were prepared as described above, except that EDTA was omitted from the gel-loading buffer. Samples were electrophoresed through an 8% acrylamide gel containing 50 μM Phos-tag–acrylamide and 100 μM $MnCl_2$. After electrophoresis, the gel was washed in transfer buffer with 2 mM EDTA for 20 min followed by 1 mM EDTA for 10 min and 10 min with transfer buffer as described previously (11). Proteins were transferred to Immobilon-P membranes and analyzed as described above.

Microscopy. For assessment of meiotic progression, cells that had been incubated in sporulation medium for 36 h were fixed with ethanol, stained with DAPI, and photographed under wet mount conditions using a Nikon Optiphot equipped for epifluorescence as previously described (8). Sporulation efficiency was analyzed by phase-contrast microscopy.

SUPPLEMENTAL MATERIAL

Supplemental material is available online only.

SUPPLEMENTAL FILE 1, XLSX file, 2.8 MB.

ACKNOWLEDGMENTS

We thank Thomas Beer and Hsin-Yao Tang (Wistar Proteomics and Metabolomics Facility) for their advice and assistance with the MS analyses and Julia Lee-Soety for valuable discussions and comments on the manuscript.

This work was supported by a grant from the NIH (GM120090) to E.W.

REFERENCES

1. Neiman AM. 2011. Sporulation in the budding yeast *Saccharomyces cerevisiae*. Genetics 189:737–765. https://doi.org/10.1534/genetics.111.127126.
2. Chu S, DeRisi J, Eisen M, Mulholland J, Botstein D, Brown PO, Herskowitz I. 1998. The transcriptional program of sporulation in budding yeast. Science 282:699–705. https://doi.org/10.1126/science.282.5389.699. [Published erratum appears in Science 1998 Nov 20;282(5393):1421.].
3. Primig M, Williams R, Winzeler E, Tevzadze G, Conway A, Hwang S, Davis R, Esposito R. 2000. The core meiotic transcriptome in budding yeasts. Nat Genet 26:415–423. https://doi.org/10.1038/82539.
4. Chu S, Herskowitz I. 1998. Gametogenesis in yeast is regulated by a transcriptional cascade dependent on Ndt80. Mol Cell 1:685–696. https://doi.org/10.1016/s1097-2765(00)80068-4.
5. Hepworth SR, Friesen H, Segall J. 1998. *NDT80* and the meiotic recombination checkpoint regulate expression of middle sporulation-specific genes in *Saccharomyces cerevisiae*. Mol Cell Biol 18:5750–5761. https://doi.org/10.1128/mcb.18.10.5750.
6. Winter E. 2012. The Sum1/Ndt80 transcriptional switch and commitment to meiosis in *Saccharomyces cerevisiae*. Microbiol Mol Biol Rev 76:1–15. https://doi.org/10.1128/MMBR.05010-11.
7. Neiman AM. 2005. Ascospore formation in the yeast *Saccharomyces cerevisiae*. Microbiol Mol Biol Rev 69:565–584. https://doi.org/10.1128/MMBR.69.4.565-584.2005.
8. Krisak L, Strich R, Winters RS, Hall JP, Mallory MJ, Kreitzer D, Tuan RS, Winter E. 1994. Smk1, a developmentally regulated MAP kinase, is required for spore wall assembly in *Saccharomyces cerevisiae*. Genes Dev 8:2151–2161. https://doi.org/10.1101/gad.8.18.2151.
9. Wagner M, Briza P, Pierce M, Winter E. 1999. Distinct steps in yeast spore morphogenesis require distinct Smk1 MAP kinase thresholds. Genetics 151:1327–1340.
10. Wagner M, Pierce M, Winter E. 1997. The CDK-activating kinase Cak1 can dosage suppress sporulation defects of Smk1 MAP kinase mutants and is required for spore wall morphogenesis in *Saccharomyces cerevisiae*. EMBO J 16:1305–1317. https://doi.org/10.1093/emboj/16.6.1305.
11. Whinston E, Omerza G, Singh A, Tio CW, Winter E. 2013. Activation of the Smk1 mitogen-activated protein kinase by developmentally regulated autophosphorylation. Mol Cell Biol 33:e00408-16. https://doi.org/10.1128/MCB.00973-12.
12. Schaber M, Lindgren A, Schindler K, Bungard D, Kaldis P, Winter E. 2002. *CAK1* promotes meiosis and spore formation in *Saccharomyces cerevisiae* in a *CDC28*-independent fashion. Mol Cell Biol 22:57–68. https://doi.org/10.1128/mcb.22.1.57-68.2002.
13. Tio CW, Omerza G, Phillips T, Lou HJ, Turk BE, Winter E. 2017. Ssp2 binding activates the Smk1 mitogen-activated protein kinase. Mol Cell Biol 37 https://doi.org/10.1128/MCB.00607-16.
14. Tio CW, Omerza G, Sunder S, Winter E. 2015. Autophosphorylation of the Smk1 MAPK is spatially and temporally regulated by Ssp2 during meiotic development in yeast. Mol Biol Cell 26:3546–3555. https://doi.org/10.1091/mbc.E15-05-0322.
15. Berchowitz LE, Gajadhar AS, van Werven FJ, De Rosa AA, Samoylova ML, Brar GA, Xu Y, Xiao C, Futcher B, Weissman JS, White FM, Amon A. 2013. A developmentally regulated translational control pathway establishes the meiotic chromosome segregation pattern. Genes Dev 27:2147–2163. https://doi.org/10.1101/gad.224253.113.
16. Berchowitz LE, Kabachinski G, Walker MR, Carlile TM, Gilbert WV, Schwartz TU, Amon A. 2015. Regulated formation of an amyloid-like translational repressor governs gametogenesis. Cell 163:406–418. https://doi.org/10.1016/j.cell.2015.08.060.
17. Carpenter K, Bell RB, Yunus J, Amon A, Berchowitz LE. 2018. Phosphorylation-mediated clearance of amyloid-like assemblies in meiosis. Dev Cell 45:392–405.e6. https://doi.org/10.1016/j.devcel.2018.04.001.
18. Omerza G, Tio CW, Philips T, Diamond A, Neiman AM, Winter E. 2018. The meiosis-specific Cdc20 family-member Ama1 promotes binding of the Ssp2 activator to the Smk1 MAP kinase. Mol Biol Cell 29:66–74. https://doi.org/10.1091/mbc.E17-07-0473.
19. McDonald CM, Cooper KF, Winter E. 2005. The Ama1-directed anaphase-promoting complex regulates the Smk1 mitogen-activated protein kinase during meiosis in yeast. Genetics 171:901–911. https://doi.org/10.1534/genetics.105.045567.
20. Okaz E, Arguello-Miranda O, Bogdanova A, Vinod PK, Lipp JJ, Markova Z, Zagoriy I, Novak B, Zachariae W. 2012. Meiotic prophase requires proteolysis of M phase regulators mediated by the meiosis-specific APC/C-Ama1. Cell 151:603–618. https://doi.org/10.1016/j.cell.2012.08.044.
21. Oelschlaegel T, Schwickart M, Matos J, Bogdanova A, Camasses A, Havlis J, Shevchenko A, Zachariae W. 2005. The yeast APC/C subunit Mnd2 prevents premature sister chromatid separation triggered by the meiosis-specific APC/C-Ama1. Cell 120:773–788. https://doi.org/10.1016/j.cell.2005.01.032.
22. Penkner AM, Prinz S, Ferscha S, Klein F. 2005. Mnd2, an essential antagonist of the anaphase-promoting complex during meiotic prophase. Cell 120:789–801. https://doi.org/10.1016/j.cell.2005.01.017.
23. Cooper KF, Mallory MJ, Egeland DB, Jarnik M, Strich R. 2000. Ama1p is a meiosis-specific regulator of the anaphase promoting complex/cyclosome in yeast. Proc Natl Acad Sci U S A 97:14548–14553. https://doi.org/10.1073/pnas.250351297.
24. Arguello-Miranda O, Zagoriy I, Mengoli V, Rojas J, Jonak K, Oz T, Graf P, Zachariae W. 2017. Casein kinase 1 coordinates cohesin cleavage, gametogenesis, and exit from M phase in meiosis II. Dev Cell 40:37–52. https://doi.org/10.1016/j.devcel.2016.11.021.
25. Wang F, Zhang R, Feng W, Tsuchiya D, Ballew O, Li J, Denic V, Lacefield S. 2020. Autophagy of an amyloid-like translational repressor regulates meiotic exit. Dev Cell 52:141–151.e5. https://doi.org/10.1016/j.devcel.2019.12.017.
26. Diamond AE, Park JS, Inoue I, Tachikawa H, Neiman AM. 2009. The anaphase promoting complex targeting subunit Ama1 links meiotic exit to cytokinesis during sporulation in *Saccharomyces cerevisiae*. Mol Biol Cell 20:134–145. https://doi.org/10.1091/mbc.e08-06-0615.
27. Tagwerker C, Flick K, Cui M, Guerrero C, Dou Y, Auer B, Baldi P, Huang L, Kaiser P. 2006. A tandem affinity tag for two-step purification under fully denaturing conditions: application in ubiquitin profiling and protein complex identification combined with in vivo cross-linking. Mol Cell Proteomics 5:737–748. https://doi.org/10.1074/mcp.M500368-MCP200.
28. Mazur P, Morin N, Baginsky W, el-Sherbeini M, Clemas JA, Nielsen JB, Foor F. 1995. Differential expression and function of two homologous subunits of yeast 1,3-beta-D-glucan synthase. Mol Cell Biol 15:5671–5681. https://doi.org/10.1128/mcb.15.10.5671.
29. Felder T, Bogengruber E, Tenreiro S, Ellinger A, Sa-Correia I, Briza P. 2002. Dtrlp, a multidrug resistance transporter of the major facilitator superfamily, plays an essential role in spore wall maturation in *Saccharomyces cerevisiae*. Eukaryot Cell 1:799–810. https://doi.org/10.1128/ec.1.5.799-810.2002.
30. Pan HP, Wang N, Tachikawa H, Gao XD, Nakanishi H. 2018. Osw2 is required for proper assembly of glucan and/or mannan layers of the yeast spore wall. J Biochem 163:293–304. https://doi.org/10.1093/jb/mvx082.
31. Huang LS, Doherty HK, Herskowitz I. 2005. The Smk1p MAP kinase negatively regulates Gsc2p, a 1,3-beta-glucan synthase, during spore wall morphogenesis in *Saccharomyces cerevisiae*. Proc Natl Acad Sci U S A 102:12431–12436. https://doi.org/10.1073/pnas.0502324102.
32. Hall MC, Torres MP, Schroeder GK, Borchers CH. 2003. Mnd2 and Swm1 are core subunits of the *Saccharomyces cerevisiae* anaphase-promoting complex. J Biol Chem 278:16698–16705. https://doi.org/10.1074/jbc.M213109200.
33. Schwickart M, Havlis J, Habermann B, Bogdanova A, Camasses A, Oelschlaegel T, Shevchenko A, Zachariae W. 2004. Swm1/Apc13 is an evolutionarily conserved subunit of the anaphase-promoting complex stabilizing the association of Cdc16 and Cdc27. Mol Cell Biol 24:3562–3576. https://doi.org/10.1128/mcb.24.8.3562-3576.2004.
34. Ufano S, San-Segundo P, del Rey F, Vázquez de Aldana CR. 1999. *SWM1*, a developmentally regulated gene, is required for spore wall assembly in *Saccharomyces cerevisiae*. Mol Cell Biol 19:2118–2129. https://doi.org/10.1128/mcb.19.3.2118.
35. Jin L, Zhang K, Sternglanz R, Neiman AM. 2017. Predicted RNA binding proteins Pes4 and Mip6 regulate mRNA levels, translation, and localization during sporulation in budding yeast. Mol Cell Biol 37:e00408-16. https://doi.org/10.1128/MCB.00408-16.
36. Kobayashi T, Hotta Y, Tabata S. 1993. Isolation and characterization of a yeast gene that is homologous with a meiosis-specific cDNA from a plant. Mol Gen Genet 237:225–232. https://doi.org/10.1007/BF00282804.
37. Sari F, Heinrich M, Meyer W, Braus GH, Irniger S. 2008. The C-terminal region of the meiosis-specific protein kinase Ime2 mediates protein instability and is required for normal spore formation in budding

yeast. J Mol Biol 378:31–43. https://doi.org/10.1016/j.jmb.2008.02.001.
38. Phillips T, Tio CW, Omerza G, Rimal A, Lokareddy RK, Cingolani G, Winter E. 2018. RNA recognition-like motifs activate a mitogen-activated protein kinase. Biochemistry 57:6878–6887. https://doi.org/10.1021/acs.biochem.8b01032.
39. Tan GS, Lewandowski R, Mallory MJ, Strich R, Cooper KF. 2013. Mutually dependent degradation of Ama1p and Cdc20p terminates APC/C ubiquitin ligase activity at the completion of meiotic development in yeast. Cell Div 8:9. https://doi.org/10.1186/1747-1028-8-9.
40. Tan GS, Magurno J, Cooper KF. 2011. Ama1p-activated anaphase-promoting complex regulates the destruction of Cdc20p during meiosis II. Mol Biol Cell 22:315–326. https://doi.org/10.1091/mbc.E10-04-0360.
41. Brar GA, Yassour M, Friedman N, Regev A, Ingolia NT, Weissman JS. 2012. High-resolution view of the yeast meiotic program revealed by ribosome profiling. Science 335:552–557. https://doi.org/10.1126/science.1215110.
42. Wang F, Denic V, Lacefield S. 2020. Autophagy prevents runaway meiotic divisions. Autophagy 16:969–970. https://doi.org/10.1080/15548627.2020.1739449.
43. Kimata Y. 2019. APC/C ubiquitin ligase: coupling cellular differentiation to G1/G0 phase in multicellular systems. Trends Cell Biol 29:591–603. https://doi.org/10.1016/j.tcb.2019.03.001.
44. Holt LJ, Hutti JE, Cantley LC, Morgan DO. 2007. Evolution of Ime2 phosphorylation sites on Cdk1 substrates provides a mechanism to limit the effects of the phosphatase Cdc14 in meiosis. Mol Cell 25:689–702. https://doi.org/10.1016/j.molcel.2007.02.012.
45. Tagwerker C, Zhang H, Wang X, Larsen LS, Lathrop RH, Hatfield GW, Auer B, Huang L, Kaiser P. 2006. HB tag modules for PCR-based gene tagging and tandem affinity purification in *Saccharomyces cerevisiae*. Yeast 23:623–632. https://doi.org/10.1002/yea.1380.
46. Bahler J, Wu JQ, Longtine MS, Shah NG, McKenzie A, III, Steever AB, Wach A, Philippsen P, Pringle JR. 1998. Heterologous modules for efficient and versatile PCR-based gene targeting in *Schizosaccharomyces pombe*. Yeast 14:943–951. https://doi.org/10.1002/(SICI)1097-0061(199807)14:10<943::AID-YEA292>3.0.CO;2-Y.
47. Winzeler EA, Shoemaker DD, Astromoff A, Liang H, Anderson K, Andre B, Bangham R, Benito R, Boeke JD, Bussey H, Chu AM, Connelly C, Davis K, Dietrich F, Dow SW, El Bakkoury M, Foury F, Friend SH, Gentalen E, Giaever G, Hegemann JH, Jones T, Laub M, Liao H, Liebundguth N, Lockhart DJ, Lucau-Danila A, Lussier M, M'Rabet N, Menard P, Mittmann M, Pai C, Rebischung C, Revuelta JL, Riles L, Roberts CJ, Ross-MacDonald P, Scherens B, Snyder M, Sookhai-Mahadeo S, Storms RK, Veronneau S, Voet M, Volckaert G, Ward TR, Wysocki R, Yen GS, Yu K, Zimmermann K, Philippsen P, et al. 1999. Functional characterization of the *S. cerevisiae* genome by gene deletion and parallel analysis. Science 285:901–906. https://doi.org/10.1126/science.285.5429.901.
48. Schindler K, Winter E. 2006. Phosphorylation of Ime2 regulates meiotic progression in *Saccharomyces cerevisiae*. J Biol Chem 281:18307–18316. https://doi.org/10.1074/jbc.M602349200.
49. Kaiser P, Meierhofer D, Wang X, Huang L. 2008. Tandem affinity purification combined with mass spectrometry to identify components of protein complexes. Methods Mol Biol 439:309–326. https://doi.org/10.1007/978-1-59745-188-8_21.
50. Knop M, Siegers K, Pereira G, Zachariae W, Winsor B, Nasmyth K, Schiebel E. 1999. Epitope tagging of yeast genes using a PCR-based strategy: more tags and improved practical routines. Yeast 15:963–972. https://doi.org/10.1002/(SICI)1097-0061(199907)15:10B<963::AID-YEA399>3.0.CO;2-W.